OQ^{2}AM – Optical QAM scheme with orthogonal polarization

Robert Fritsch, Joachim Speidel
Institut für Nachrichtenübertragung, Pfaffenwaldring 47, Universität Stuttgart
+49 / (0)711 / 685-8016, -7929, {fritsch,speidel}@inue.uni-stuttgart.de

Abstract

We present a novel optical quadrature modulation scheme, which applies a QAM on two Laser output signals with orthogonal polarization (OQ^{2}AM). Transmitter and receiver with heterodyne principle are described. The performance of the scheme is investigated in the presence of Laser phase noise, group velocity and polarization mode distortion of the fiber.

I. Introduction

Main target of research on optical communications systems is the increase of bit rates from about 40 to 160 Gbit/s. One method is to use modulation formats with more than two levels to increase spectral efficiency [1]–[3]. In the electrical domain, e. g. mobile communications, quadrature amplitude modulation (QAM) is frequently used [4]. Inphase and quadrature component built up a two dimensional signal constellation. Phase shift keying (PSK) is a subset of QAM and included in the following considerations. In the optical domain, we can use an additional, optical carrier with orthogonal polarization. If we apply in this second constellation plane a QAM as well, we get a four dimensional constellation, which we call optical quadrature QAM or OQ^{2}AM.

II. OQ^{2}AM transmitter and receiver

In Fig. 1 the principle OQ^{2}AM transmitter and receiver are depicted. The electrical bit sequence a_k is input into a mapper which allocates $2M$ subsequent bits to a symbol vector $\vec{\underline{b}}_m = (\underline{b}_{\mathrm{x},m}\ \underline{b}_{\mathrm{y},m})^\mathrm{T}$. Underlines denote complex signals. Each component can take on 2^M positions in the complex domain. Thus, $\vec{\underline{b}}_m$ can take on 2^{2M} values. Consequently, the bit rate and the spectral efficiency are doubled compared to QAM with only one polarization. The symbols are the electrical input signals to the optical QAM modulators (OQAM). The OQAMs are driven by linear polarized light of a CW-Laser with wavelength $\lambda_0 = \frac{2\pi c}{\omega_0}$. The light is split into two parts. The polarization of the first one is shifted by $90°$. Thus, the upper OQAM modulates with the linear x-polarized optical field $e_0\vec{e}_\mathrm{x}$ with $e_0 = E_0\cos(\omega_0 t + \varphi_0)$ and the lower OQAM with the linear y-polarized optical field

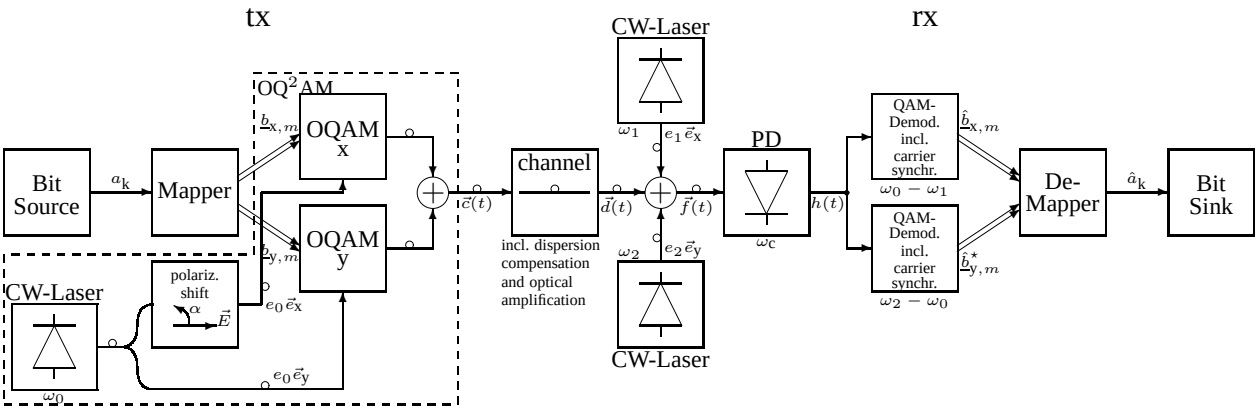

Fig. 1: Transmitter and receiver for OQ^{2}AM

$e_0\vec{e}_{\mathrm{y}}$. An example of the OQAM device is described in section IV. The electrical field strength at the output of the transmitter is

$$\vec{c}(t) = \mathrm{Re}\Bigg\{ \underbrace{E_0 \mathrm{e}^{\mathrm{j}(\omega_0 t+\varphi_0)}}_{\text{CW-Laser}} \overbrace{\sum_{m=-\infty}^{\infty} \underbrace{\mathrm{w}(t-mT)}_{\text{impulse}} \underline{\vec{b}}_m}^{\underline{\vec{g}}(t)} \Bigg\}, \text{ with } \underline{\vec{b}}_m = \begin{pmatrix} \underline{b}_{\mathrm{x},m} \\ \underline{b}_{\mathrm{y},m} \end{pmatrix} \text{ and } \underline{\vec{g}}(t) = \begin{pmatrix} \underline{g}_{\mathrm{x}}(t) \\ \underline{g}_{\mathrm{y}}(t) \end{pmatrix}. \quad (1)$$

The impulse $\mathrm{w}(t)$ of the OQAM modulator is band limited with $\omega_{\mathrm{c}}^{\mathrm{w}}$.

At the receiver two CW-Laser signals with wavelengths $\lambda_1 = \frac{2\pi c}{\omega_1}$ and $\lambda_2 = \frac{2\pi c}{\omega_2}$ and the polarization directions $\vec{e}_{\mathrm{x}}$ and $\vec{e}_{\mathrm{y}}$ are added to the received signal $\vec{d}(t)$. The heterodyne principle is used. Thus we obtain

$$\vec{f}(t) = \begin{pmatrix} f_{\mathrm{x}}(t) \\ f_{\mathrm{y}}(t) \end{pmatrix} = \vec{d}(t) + \mathrm{Re}\left\{ E_1 \mathrm{e}^{\mathrm{j}(\omega_1 t+\varphi_1)} \vec{e}_{\mathrm{x}} + E_2 \mathrm{e}^{\mathrm{j}(\omega_2 t+\varphi_2)} \vec{e}_{\mathrm{y}} \right\}. \quad (2)$$

Note that $\vec{d}(t)$ is real.

To show the principle operation of the receiver, we assume ideal transmission, i.e. $\vec{d}(t) = \vec{c}(t)$. In section V we investigate the system performance under real channel conditions. The photodiode (PD) is modelled by $h(t) = R \cdot |\vec{f}(t)|^2 * r_{\omega_{\mathrm{c}}}(t)$, where $r_{\omega_{\mathrm{c}}}(t)$ is the impulse response of an ideal low pass filter with angular cut off frequency ω_{c}. For simplicity we set the responsivity $R = 1$. After O/E conversion we get with (1) and (2)

$$\begin{aligned} h(t) = \left|\vec{f}(t)\right|^2 * r_{\omega_{\mathrm{c}}}(t) \;\; = \;\; & \mathrm{Re}\Bigg\{ \underbrace{E_0 E_1 \underline{g}_{\mathrm{x}}(t) \mathrm{e}^{\mathrm{j}[(\omega_0-\omega_1)t+\varphi_0-\varphi_1]}}_{\text{QAM signal at } \omega_0-\omega_1} + \underbrace{E_0 E_2 \underline{g}_{\mathrm{y}}^{\star}(t) \mathrm{e}^{\mathrm{j}[(\omega_2-\omega_0)t+\varphi_2-\varphi_0]}}_{\text{QAM signal at } \omega_2-\omega_0} \Bigg\} \\ & + \frac{E_0^2}{2} \left(\underline{g}_{\mathrm{x}}(t) \underline{g}_{\mathrm{x}}^{\star}(t) + \underline{g}_{\mathrm{y}}(t) \underline{g}_{\mathrm{y}}^{\star}(t) \right) + \frac{E_1^2 + E_2^2}{2}. \end{aligned} \quad (3)$$

$*$ denotes convolution and $\star$ conjugate complex operation. Obviously, the electrical signal $h(t)$ consists of two QAM signals in the frequency range $\omega_0 - \omega_1$ and $\omega_2 - \omega_0$, resp. as well as a baseband signal and a dc value. $h(t)$ can be demodulated by two electrical QAM-Demodulators in Fig. 1. The resulting estimates $\hat{\underline{b}}_{\mathrm{x,m}}$ and $\hat{\underline{b}}_{\mathrm{y,m}}^{\star}$ can be demapped to the estimated bit sequence $\hat{a}_{\mathrm{k}}$.

III. Homodyne Receiver Structure

Fig. 2 shows an alternative receiver structure. The homodyne principle is used. The two polarization directions $\vec{e}_{\mathrm{x}}$ and $\vec{e}_{\mathrm{y}}$ of the electrical field are detected separately by the circuit in Fig. 2(b). Thereby each normal and quadrature component is demodulated separately as well. Index "n" denotes the normal and index "q" the quadrature component. For demodulation the two coherent laser signals $e_1\vec{e}_i$ with $e_1 = E_1 \cos(\omega_0 t + \varphi_0)$ and $\tilde{e}_1\vec{e}_i$ with $\tilde{e}_1 = -E_1 \sin(\omega_0 t + \varphi_0)$ are added to the received signal $\vec{d}(t)$. Thus we obtain

$$\begin{aligned} \vec{f}_{i,\mathrm{n}}(t) &= \mathrm{Re}\left\{ \vec{d}(t) + E_0 \mathrm{e}^{\mathrm{j}(\omega_0 t+\varphi_0)} \right\} \\ \vec{f}_{i,\mathrm{q}}(t) &= \mathrm{Re}\left\{ \vec{d}(t) + E_0 \mathrm{e}^{\mathrm{j}(\omega_0 t+\varphi_0+\pi/2)} \right\} \end{aligned}, \; i = \mathrm{x}, \mathrm{y} \quad (4)$$

To show the principle operation of the homodyne receiver, we also assume ideal transmission, i.e. $\vec{d}(t) = \vec{c}(t)$. After O/E conversion we get with (1) and (4)

$$\begin{aligned} \tilde{h}_{i,\mathrm{n}}(t) &= \left|\vec{f}_{i,\mathrm{n}}\right|^2 * r_{\omega_{\mathrm{c}}}(t) = E_0 E_1 g_{i,\mathrm{n}}(t) + \tfrac{E_1^2}{2} + \tfrac{E_0^2}{2} \left(\underline{g}_{\mathrm{x}}(t) \underline{g}_{\mathrm{x}}^{\star}(t) + \underline{g}_{\mathrm{y}}(t) \underline{g}_{\mathrm{y}}^{\star}(t) \right) \\ \tilde{h}_{i,\mathrm{q}}(t) &= \left|\vec{f}_{i,\mathrm{q}}\right|^2 * r_{\omega_{\mathrm{c}}}(t) = E_0 E_1 g_{i,\mathrm{q}}(t) + \tfrac{E_1^2}{2} + \tfrac{E_0^2}{2} \left(\underline{g}_{\mathrm{x}}(t) \underline{g}_{\mathrm{x}}^{\star}(t) + \underline{g}_{\mathrm{y}}(t) \underline{g}_{\mathrm{y}}^{\star}(t) \right) \end{aligned} \quad (5)$$

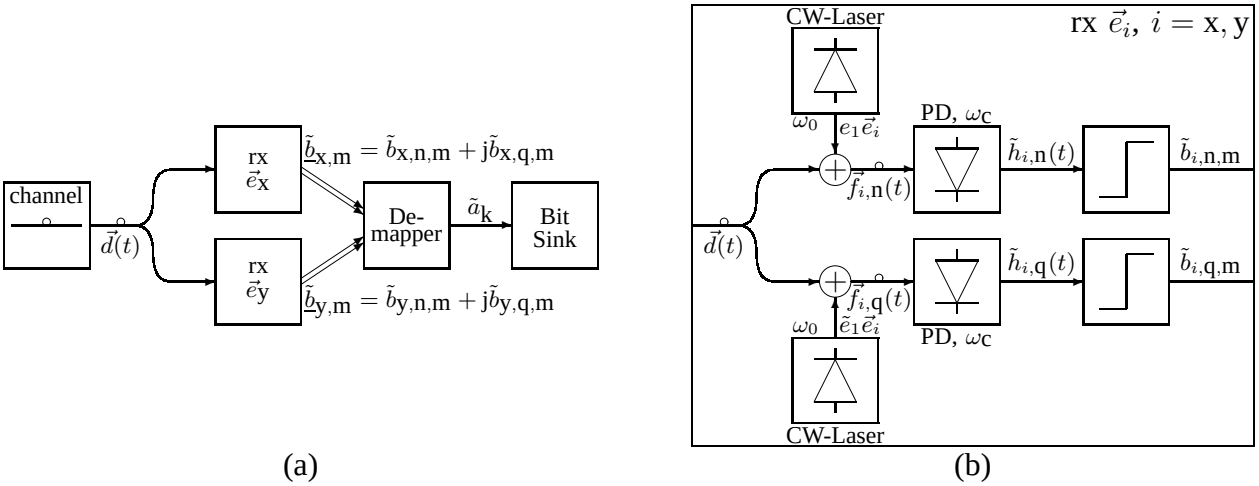

Fig. 2: Alternative receiver with homodyne principle, (a) complete receiver, (b) detail of rx $\vec{e}_\mathrm{x}$ and $\vec{e}_\mathrm{y}$

where we have defined $\underline{g}_i(t) = g_{i,\mathrm{n}} + \mathrm{j}g_{i,\mathrm{q}}$, $i = \mathrm{x,y}$

$\tilde{h}_{i,\mathrm{n}}(t)$ and $\tilde{h}_{i,\mathrm{q}}(t)$ contain the transmitted baseband signals $g_{i,\mathrm{n}}(t)$ and $g_{i,\mathrm{q}}(t)$, but also in the same spectral range the disturbing signals $\underline{g}_\mathrm{x}$ and $\underline{g}_\mathrm{y}$. To reduce this distortion $E_1 \gg E_0$ can be chosen. In this case

$$\begin{aligned} \tilde{h}_{i,\mathrm{n}}(t) &\simeq E_0 E_1 g_{i,\mathrm{n}}(t) + \tfrac{E_1^2}{2} \\ \tilde{h}_{i,\mathrm{q}}(t) &\simeq E_0 E_1 g_{i,\mathrm{q}}(t) + \tfrac{E_1^2}{2} \end{aligned} \quad \text{for } E_1 \gg E_0 \tag{6}$$

results. However (6) still contains a large dc value which reduces the dynamic range of the components and as a consequence the performance of the system.

The stringent condition $E_1 \gg E_0$ has to be met also in case of $g_\mathrm{y}(t) = 0$, i.e. no orthogonal polarized signal is transmitted. This drawback is not present for a heterodyne receiver. However, the cut-off frequency of the PD for the homodyne receiver is at least by factor 6 lower than with the heterodyne principle in Fig. 1. On the other hand, the homodyne receiver requires 4 lasers and 4 PD whereas for the heterodyne receiver only two lasers and one PD are required.

IV. OQAM MODULATION WITH DIFFERENTIAL (DUAL-SPLIT ELECTRODE) MACH ZEHNDER MODULATOR

Fig. 3 shows the principle structure of an OQAM modulator. The normal and quadrature component are modulated separately by optical amplitude modulators (OAM). To obtain the proper relation of phase at the summation node, the lower path has to be shifted by $3\pi/2$ in phase. This will compensate the phase shift of the first cross coupler. The second cross coupler will add the normal and quadrature component with a phase shift of $\pi/2$. For simplicity the cross couplers are assumed to be lossless.

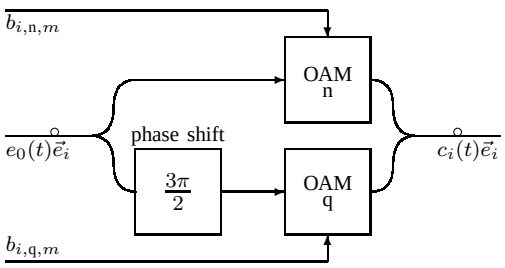

Fig. 3: Priciple structure of a OQAM modulator; $i = \mathrm{x,y}$

In Fig. 4 the principle structure of the OAM is depicted. From [5], [6] the principle output signal of the differential Mach Zehnder (MZ) modulator can be written as

$$c_{i,k}(t) = \mathrm{Re}\left\{ \frac{1}{\sqrt{2}\alpha} \underbrace{E_0 \mathrm{e}^{\mathrm{j}(\omega_0 t+\varphi_0)}}_{e_0} \left[\underbrace{Y_\mathrm{u}}_{1/\sqrt{2}} \mathrm{e}^{\mathrm{j}\pi\left(\frac{u_{\mathrm{rf},i,k,\mathrm{u}}(t)}{U_{\mathrm{pi},i,k,\mathrm{rf}}(\vartheta)}+\frac{U_{\mathrm{dc},i,k,\mathrm{u}}}{U_{\mathrm{pi},i,k,\mathrm{dc}}(\vartheta)}\right)} + \underbrace{Y_\mathrm{l}}_{1/\sqrt{2}} \mathrm{e}^{-\mathrm{j}\pi\left(\frac{u_{\mathrm{rf},i,k,\mathrm{l}}(t)}{U_{\mathrm{pi},i,k,\mathrm{rf}}(\vartheta)}+\frac{U_{\mathrm{dc},i,k,\mathrm{l}}}{U_{\mathrm{pi},i,k,\mathrm{dc}}(\vartheta)}\right)} \right] \right\}. \tag{7}$$

$i = \mathrm{x}, \mathrm{y}$; $k = \mathrm{n}, \mathrm{q}$ and α is the insertion loss of the modulator. The upper and lower split ratios are $Y_u = Y_l = 1/\sqrt{2}$ for a perfect Mach Zehnder modulator. We recommend the use of temperature compensation to achieve $U_{\mathrm{pi},i,k,o}(\vartheta) = \text{const}$, $o = \mathrm{rf}, \mathrm{dc}$. For amplitude modulation

$$\begin{aligned} &\frac{u_{\mathrm{rf},i,k,\mathrm{u}}(t)}{U_{\mathrm{pi},i,k,\mathrm{rf}}} = \frac{u_{\mathrm{rf},i,k,\mathrm{l}}(t)}{U_{\mathrm{pi},i,k,\mathrm{rf}}} = u_{i,k}(t) \in [-\tfrac{1}{4}, \tfrac{1}{4}] \text{ and} \\ &\frac{U_{\mathrm{dc},i,k,\mathrm{u}}}{U_{\mathrm{pi},i,k,\mathrm{dc}}} = -\frac{U_{\mathrm{dc},i,k,\mathrm{l}}}{U_{\mathrm{pi},i,k,\mathrm{dc}}} = -\tfrac{1}{2} \end{aligned} \tag{8}$$

can be chosen. Thus

$$c_{i,k}(t) = \frac{E_0}{\alpha} \mathrm{Re}\left\{ \mathrm{e}^{\mathrm{j}(\omega_0 t+\varphi_0)} \cos\left(\pi u_{i,k}(t) - \frac{\pi}{2}\right) \right\}. \tag{9}$$

In Fig. 4 the upper and lower pre equalizer have to equalize the upper and lower input characteristic resp., furthermore the cos edge equalizer has to equalize the cosine distortion in (9). Thus including the impulse shaping filter we get

$$c_{i,k}(t) = \frac{E_0}{\alpha} \cos(\omega_0 t + \varphi_0) \sum_{m=-\infty}^{\infty} \mathrm{w}(t - mT) b_{i,k,m}. \tag{10}$$

This signals are combined as in Fig. 3 and Fig. 1 and for $\alpha = 1$ we get (1).

V. Performance of OQ^{2}AM

A. Performance of OQ^{2}AM compared to polarization multiplexed OQAM (PMOQAM)

The system in Fig. 1 can also be considered as a PMOQAM. On each of the two orthogonal polarization paths $\vec{e}_\mathrm{x}$ and $\vec{e}_\mathrm{y}$ of the electrical field strength an OQAM signal is transmitted independently. Thereby the signal constellations of the QAMs can be chosen in the complex plane. This is a two dimensional packing problem with boundary conditions [8]. On the other hand the scheme in Fig. 1 can also be considered in general as an OQ^{2}AM. In this case the signal constellation can be

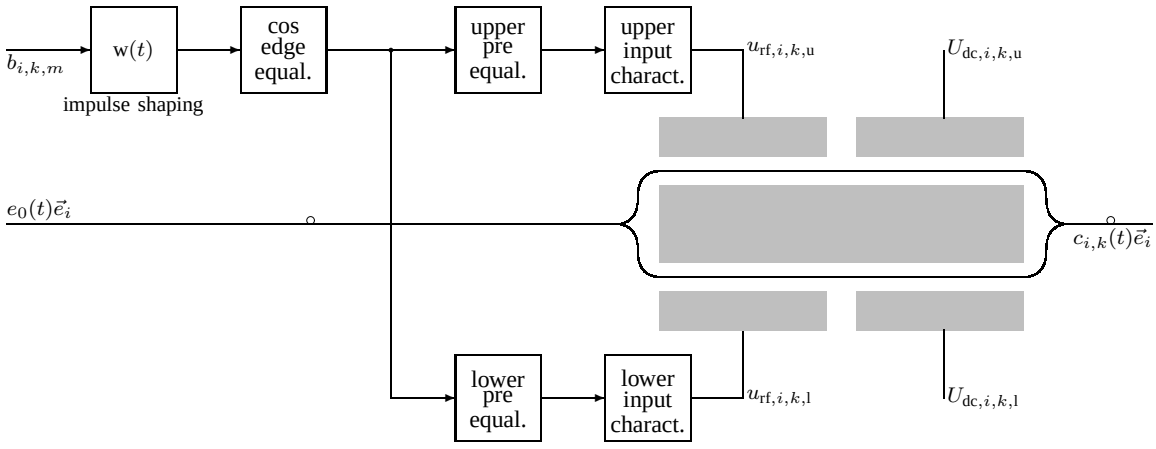

Fig. 4: Principle structure of a OAM with a differential MZ-Modulator; $i = \mathrm{x}, \mathrm{y}$; $k = \mathrm{n}, \mathrm{q}$

chosen in the four dimensional space. Allocation of signal points $\vec{b}_m$ is a four dimensional packing problem with boundary conditions [9]. Hence, PMOQAM is a special case of OQ^{2}AM.

For comparison the signal constellations with dense grid and rectangular grid are listed in Tab. I . Particularly for OQ^{2}AM they are different from [9]. We choose signal constellations out of the dense infinite packing. PMOQAM contains two independent QAM signal constellations for x and y polarization.

To increase speed of simulation for symbol error ratio SER the channel is modelled by additive white gaussian noise only. Fig. 5 shows the SER of these constellations. The OQ^{2}AM constellation outperforms the others by about 1 dB. In Fig. 5(b) the SER curves for 4 signal points are congruent. In case of 8 and 16 signal points the rectangular grid PMOQAM outperforms the dense grid. For higher modulation levels it's visa versa. Heuristically, the dense grid seems to be better. But the neglected boundary conditions for optimum signal constellations can change this, particularly for small modulation levels [8]. This also holds for the dense grid OQ^{2}AM.

B. Impact of Laser spectra and polarization mode dispersion (PMD)

We have simulated the system in Fig. 1. The CW-Laser outputs are modelled by [7].

$$e(t) = \cos(\omega t + \varphi) \text{ with } \varphi = \int \omega_\varphi(\tau)\,\mathrm{d}\tau \text{ and } \omega_\varphi(t) \text{ gaussian distributed with } \sigma^2 = 2\pi\Delta f. \tag{11}$$

Δf is the full width at half maximum of the optical Laser spectrum. $2M = 4$ signal points are choosen for the OQAMs as an example. Thus 4 bits are transmitted with each symbol. This gives a spectral efficiency of $\frac{2M}{1+\beta} = \frac{4}{(1+\beta)}\frac{\text{bit/s}}{\text{Hz}}$ where β is the roll-off factor of the pulse shaping Nyquist lowpass filter. The fiber channel is assumed to be linear with dispersion. The channel transfer function is assumed to be $\mathrm{e}^{-\mathrm{j}\beta''(\omega-\omega_0)^2 z/2}$ in the frequency range around ω_0, where z is the fiber length [10], [11]. The PD output is modelled by $h(t) = R \cdot |\vec{f}(t)|^2 + n(t)$. $n(t)$ is assumed to be gaussian noise with variance $\sigma^2 = \sigma_\mathrm{p}^2 + \sigma_0^2$ with $R = 63$. σ^2 is the total noise at the receiver and consists of one part $\sigma_\mathrm{p}^2 \sim p$, which depends on the input power p of the PD, and a signal

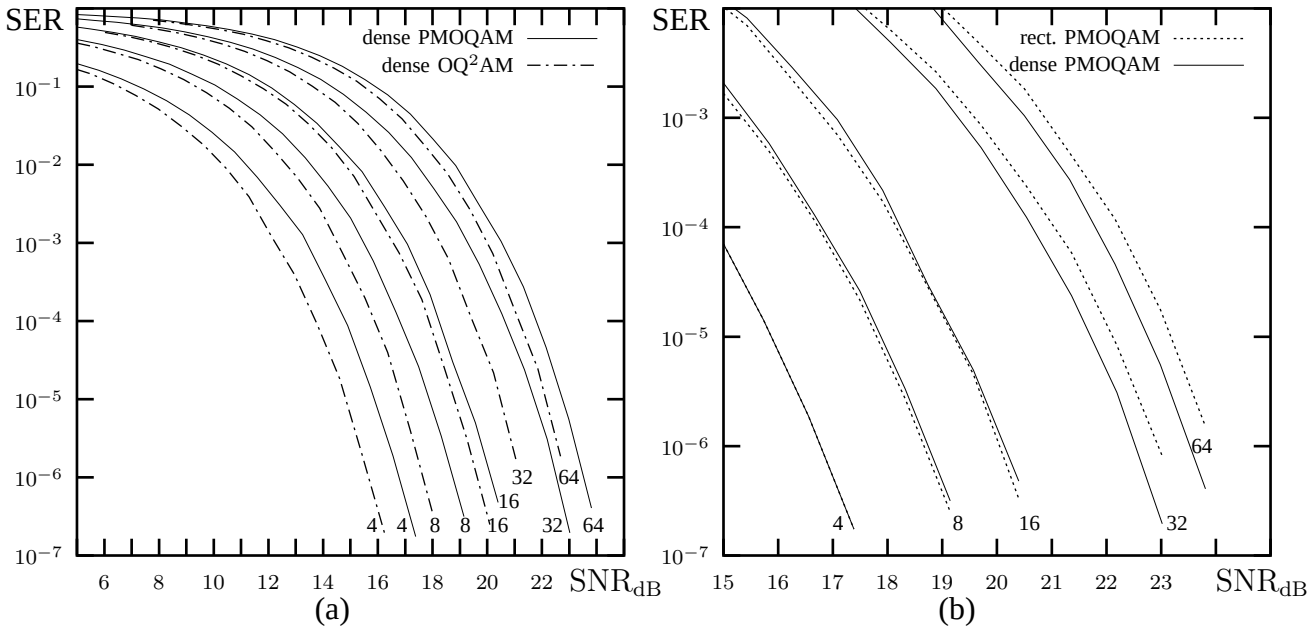

Fig. 5: Comparison of signal constellations of (a) dense grid PMOQAM with dense grid OQ^{2}AM and (b) rectangular with dense grid PMOQAM. From left to right 4,8,16,32 and 64 signal points from Tab. I are considered.

TABLE I: Signal constellations for the normal and quadrature component n,q in each polarization direction x,y

	rectangular grid PMOQAM				dense grid PMOQAM				dense grid OQ^{2}AM			
	x,n	x,q	y,n	y,q	x,n	x,q	y,n	y,q	x,n	x,q	y,n	y,q
4-Q^{2}AM	-1	0	-1	0	-1	0	-1	0	-1.155	-0.6667	-0.4714	0
	-1	0	1	0	-1	0	1	0	1.155	-0.6667	-0.4714	0
	1	0	-1	0	1	0	-1	0	0	1.333	-0.4714	0
	1	0	1	0	1	0	1	0	0	0	1.414	0
8-Q^{2}AM	-1	-1	-1	0	-0.5	-0.866	-1	0	-0.8542	-0.6576	-0.465	0.9005
	-1	-1	1	0	-0.5	-0.866	1	0	1.424	-0.6576	-0.465	0.9005
	1	-1	-1	0	1.5	-0.866	-1	0	0.2847	1.315	-0.465	0.9005
	1	-1	1	0	1.5	-0.866	1	0	0.2847	0	1.395	0.9005
	-1	1	-1	0	0.5	0.866	-1	0	-0.8542	-0.6576	0.93	-0.9005
	-1	1	1	0	0.5	0.866	1	0	-0.8542	0.6576	-0.93	-0.9005
	1	1	-1	0	-1.5	0.866	-1	0	0.2847	1.315	0.93	-0.9005
	1	1	1	0	-1.5	0.866	1	0	0.2847	-1.315	-0.93	-0.9005
16-Q^{2}AM	-1	-1	-1	-1	-0.5	-0.866	-0.5	-0.866	-0.4018	-0.6186	-0.4374	0.847
	-1	-1	1	-1	-0.5	-0.866	1.5	-0.866	1.741	-0.6186	-0.4374	0.847
	-1	-1	-1	1	-0.5	-0.866	0.5	0.866	0.6696	1.237	-0.4374	0.847
	-1	-1	1	1	-0.5	-0.866	-1.5	0.866	0.6696	0	1.312	0.847
	1	-1	-1	-1	1.5	-0.866	-0.5	-0.866	-0.4018	-0.6186	0.8748	-0.847
	1	-1	1	-1	1.5	-0.866	1.5	-0.866	-0.4018	0.6186	-0.8748	-0.847
	1	-1	-1	1	1.5	-0.866	0.5	0.866	0.6696	1.237	0.8748	-0.847
	1	-1	1	1	1.5	-0.866	-1.5	0.866	0.6696	-1.237	-0.8748	-0.847
	-1	1	-1	-1	0.5	0.866	-0.5	-0.866	1.741	-0.6186	0.8748	-0.847
	-1	1	1	-1	0.5	0.866	1.5	-0.866	1.741	0.6186	-0.8748	-0.847
	-1	1	-1	1	0.5	0.866	0.5	0.866	-1.473	0	1.312	0.847
	-1	1	1	1	0.5	0.866	-1.5	0.866	-1.473	1.237	-0.4374	0.847
	1	1	-1	-1	-1.5	0.866	-0.5	-0.866	-1.473	1.237	0.8748	-0.847
	1	1	1	-1	-1.5	0.866	1.5	-0.866	-1.473	-1.237	-0.8748	-0.847
	1	1	-1	1	-1.5	0.866	0.5	0.866	-0.4018	-1.856	1.312	0.847
	1	1	1	1	-1.5	0.866	-1.5	0.866	-0.4018	0.6186	-2.187	0.847
32-Q^{2}AM	0.1961	-0.1961	-1	-1	0.3128	0.1806	-0.5	-0.866	0	-0.6861	0.08937	1.335
	0.1961	-0.1961	1	-1	0.3128	0.1806	1.5	-0.866	2.002	-0.6861	0.08937	1.335
	0.1961	-0.1961	-1	1	0.3128	0.1806	0.5	0.866	1.001	1.047	0.08937	1.335
	0.1961	-0.1961	1	1	0.3128	0.1806	-1.5	0.866	1.001	-0.1083	1.724	1.335
	1.765	-0.1961	-1	-1	1.981	0.1806	-0.5	-0.866	0	-0.6861	1.315	-0.2472
	1.765	-0.1961	1	-1	1.981	0.1806	1.5	-0.866	0	0.4695	-0.3192	-0.2472
	1.765	-0.1961	-1	1	1.981	0.1806	0.5	0.866	1.001	1.047	1.315	-0.2472
	1.765	-0.1961	1	1	1.981	0.1806	-1.5	0.866	1.001	-1.264	-0.3192	-0.2472
	0.1961	1.373	-1	-1	1.147	1.625	-0.5	-0.866	2.002	-0.6861	1.315	-0.2472
	0.1961	1.373	1	-1	1.147	1.625	1.5	-0.866	2.002	0.4695	-0.3192	-0.2472
	0.1961	1.373	-1	1	1.147	1.625	0.5	0.866	-1.001	-0.1083	1.724	1.335
	0.1961	1.373	1	1	1.147	1.625	-1.5	0.866	-1.001	1.047	0.08937	1.335
	1.765	1.373	-1	-1	-0.5213	1.625	-0.5	-0.866	-1.001	1.047	1.315	-0.2472
	1.765	1.373	1	-1	-0.5213	1.625	1.5	-0.866	-1.001	-1.264	-0.3192	-0.2472
	1.765	1.373	-1	1	-0.5213	1.625	0.5	0.866	0	-1.842	1.724	1.335
	1.765	1.373	1	1	-0.5213	1.625	-1.5	0.866	0	0.4695	-1.545	1.335
	-1.373	-0.1961	-1	-1	-1.355	0.1806	-0.5	-0.866	0	0.4695	0.9065	-1.83
	-1.373	-0.1961	1	-1	-1.355	0.1806	1.5	-0.866	1.001	2.203	-0.3192	-0.2472
	-1.373	-0.1961	-1	1	-1.355	0.1806	0.5	0.866	1.001	-0.1083	-1.953	-0.2472
	-1.373	-0.1961	1	1	-1.355	0.1806	-1.5	0.866	1.001	-0.1083	-0.7278	-1.83
	-1.373	1.373	-1	-1	-0.5213	-1.264	-0.5	-0.866	1.001	-1.264	-1.545	1.335
	-1.373	1.373	1	-1	-0.5213	-1.264	1.5	-0.866	1.001	-1.264	0.9065	-1.83
	-1.373	1.373	-1	1	-0.5213	-1.264	0.5	0.866	-2.002	0.4695	-0.3192	-0.2472
	-1.373	1.373	1	1	-0.5213	-1.264	-1.5	0.866	-1.001	-0.1083	-1.953	-0.2472
	0.1961	-1.765	-1	-1	1.147	-1.264	-0.5	-0.866	-1.001	-0.1083	-0.7278	-1.83
	0.1961	-1.765	1	-1	1.147	-1.264	1.5	-0.866	-1.001	2.203	-0.3192	-0.2472
	0.1961	-1.765	-1	1	1.147	-1.264	0.5	0.866	0	1.625	-1.953	-0.2472
	0.1961	-1.765	1	1	1.147	-1.264	-1.5	0.866	0	1.625	-0.7278	-1.83
	-1.373	-1.765	-1	-1	-2.189	-1.264	-0.5	-0.866	-2.002	-0.6861	0.08937	1.335
	-1.373	-1.765	1	-1	-2.189	-1.264	1.5	-0.866	-2.002	-0.6861	1.315	-0.2472
	-1.373	-1.765	-1	1	-2.189	-1.264	0.5	0.866	-1.001	-1.264	-1.545	1.335
	-1.373	-1.765	1	1	-2.189	-1.264	-1.5	0.866	-1.001	-1.264	0.9065	-1.83
64-Q^{2}AM	0.1961	-0.1961	0.1961	-0.1961	0.3128	0.1806	0.3128	0.1806	0.1849	0.008214	0.05808	1.665
	0.1961	-0.1961	1.765	-0.1961	0.3128	0.1806	1.981	0.1806	2.006	0.008214	0.05808	1.665
	0.1961	-0.1961	0.1961	1.373	0.3128	0.1806	1.147	1.625	1.095	1.585	0.05808	1.665
	0.1961	-0.1961	1.765	1.373	0.3128	0.1806	-0.5213	1.625	1.095	0.5339	1.545	1.665
	0.1961	-0.1961	-1.373	-0.1961	0.3128	0.1806	-1.355	0.1806	0.1849	0.008214	1.173	0.2249
	0.1961	-0.1961	-1.373	1.373	0.3128	0.1806	-0.5213	-1.264	0.1849	1.06	-0.3136	0.2249
	0.1961	-0.1961	0.1961	-1.765	0.3128	0.1806	1.147	-1.264	1.095	1.585	1.173	0.2249
	0.1961	-0.1961	-1.373	-1.765	0.3128	0.1806	-2.189	-1.264	1.095	-0.5175	-0.3136	0.2249
	1.765	-0.1961	0.1961	-0.1961	1.981	0.1806	0.3128	0.1806	2.006	0.008214	1.173	0.2249
	1.765	-0.1961	1.765	-0.1961	1.981	0.1806	1.981	0.1806	2.006	1.06	-0.3136	0.2249
	1.765	-0.1961	0.1961	1.373	1.981	0.1806	1.147	1.625	-0.7256	0.5339	1.545	1.665
	1.765	-0.1961	1.765	1.373	1.981	0.1806	-0.5213	1.625	-0.7256	1.585	0.05808	1.665
	1.765	-0.1961	-1.373	-0.1961	1.981	0.1806	-1.355	0.1806	-0.7256	1.585	1.173	0.2249
	1.765	-0.1961	-1.373	1.373	1.981	0.1806	-0.5213	-1.264	-0.7256	-0.5175	-0.3136	0.2249
	1.765	-0.1961	0.1961	-1.765	1.981	0.1806	1.147	-1.264	0.1849	-1.043	1.545	1.665
	1.765	-0.1961	-1.373	-1.765	1.981	0.1806	-2.189	-1.264	0.1849	1.06	-1.429	1.665
	0.1961	1.373	0.1961	-0.1961	1.147	1.625	0.3128	0.1806	0.1849	1.06	0.8015	-1.215
	0.1961	1.373	1.765	-0.1961	1.147	1.625	1.981	0.1806	1.095	2.637	-0.3136	0.2249
	0.1961	1.373	0.1961	1.373	1.147	1.625	1.147	1.625	1.095	0.5339	-1.801	0.2249
	0.1961	1.373	1.765	1.373	1.147	1.625	-0.5213	1.625	1.095	0.5339	-0.6854	-1.215
	0.1961	1.373	-1.373	-0.1961	1.147	1.625	-1.355	0.1806	1.095	-0.5175	-1.429	1.665
	0.1961	1.373	-1.373	1.373	1.147	1.625	-0.5213	-1.264	1.095	-0.5175	0.8015	-1.215
	0.1961	1.373	0.1961	-1.765	1.147	1.625	1.147	-1.264	-1.636	1.06	-0.3136	0.2249
	0.1961	1.373	-1.373	-1.765	1.147	1.625	-2.189	-1.264	-0.7256	0.5339	-1.801	0.2249
	1.765	1.373	0.1961	-0.1961	-0.5213	1.625	0.3128	0.1806	-0.7256	0.5339	-0.6854	-1.215
	1.765	1.373	1.765	-0.1961	-0.5213	1.625	1.981	0.1806	-0.7256	2.637	-0.3136	0.2249
	1.765	1.373	0.1961	1.373	-0.5213	1.625	1.147	1.625	0.1849	2.111	-1.801	0.2249
	1.765	1.373	1.765	1.373	-0.5213	1.625	-0.5213	1.625	0.1849	2.111	-0.6854	-1.215
	1.765	1.373	-1.373	-0.1961	-0.5213	1.625	-1.355	0.1806	-1.636	0.008214	0.05808	1.665
	1.765	1.373	-1.373	1.373	-0.5213	1.625	-0.5213	-1.264	-1.636	0.008214	1.173	0.2249
	1.765	1.373	0.1961	-1.765	-0.5213	1.625	1.147	-1.264	-0.7256	-0.5175	-1.429	1.665
	1.765	1.373	-1.373	-1.765	-0.5213	1.625	-2.189	-1.264	-0.7256	-0.5175	0.8015	-1.215
	-1.373	-0.1961	0.1961	-0.1961	-1.355	0.1806	0.3128	0.1806	0.1849	-1.043	-1.801	0.2249
	-1.373	-0.1961	1.765	-0.1961	-1.355	0.1806	1.981	0.1806	0.1849	-1.043	-0.6854	-1.215
	-1.373	-0.1961	0.1961	1.373	-1.355	0.1806	1.147	1.625	-0.7256	-1.569	0.05808	1.665
	-1.373	-0.1961	1.765	1.373	-1.355	0.1806	-0.5213	1.625	-0.7256	-1.569	1.173	0.2249
	-1.373	-0.1961	-1.373	-0.1961	-1.355	0.1806	-1.355	0.1806	0.1849	-2.095	-0.3136	0.2249
	-1.373	-0.1961	-1.373	1.373	-1.355	0.1806	-0.5213	-1.264	1.095	-1.569	1.173	0.2249
	-1.373	-0.1961	0.1961	-1.765	-1.355	0.1806	1.147	-1.264	-1.636	1.06	0.8015	-1.215
	-1.373	-0.1961	-1.373	-1.765	-1.355	0.1806	-2.189	-1.264	-1.636	1.06	-1.429	1.665
	-1.373	1.373	0.1961	-0.1961	-0.5213	-1.264	0.3128	0.1806	0.1849	0.008214	-2.172	-1.215
	-1.373	1.373	1.765	-0.1961	-0.5213	-1.264	1.981	0.1806	2.006	1.06	0.8015	-1.215
	-1.373	1.373	0.1961	1.373	-0.5213	-1.264	1.147	1.625	-1.636	-1.043	-0.6854	-1.215
	-1.373	1.373	1.765	1.373	-0.5213	-1.264	-0.5213	1.625	-2.547	-0.5175	-0.3136	0.2249
	-1.373	1.373	-1.373	-0.1961	-0.5213	-1.264	-1.355	0.1806	-1.636	-1.043	-1.801	0.2249
	-1.373	1.373	-1.373	1.373	-0.5213	-1.264	-0.5213	-1.264	-1.636	-2.095	-0.3136	0.2249
	-1.373	1.373	0.1961	-1.765	-0.5213	-1.264	1.147	-1.264	0.1849	0.008214	2.288	-1.215
	-1.373	1.373	-1.373	-1.765	-0.5213	-1.264	-2.189	-1.264	-0.7256	0.5339	2.66	0.2249
	0.1961	-1.765	0.1961	-0.1961	1.147	-1.264	0.3128	0.1806	0.1849	-2.095	0.8015	-1.215
	0.1961	-1.765	1.765	-0.1961	1.147	-1.264	1.981	0.1806	2.006	-1.043	-0.6854	-1.215
	0.1961	-1.765	0.1961	1.373	1.147	-1.264	1.147	1.625	1.095	0.5339	2.66	0.2249
	0.1961	-1.765	1.765	1.373	1.147	-1.264	-0.5213	1.625	0.1849	-1.043	2.66	0.2249
	0.1961	-1.765	-1.373	-0.1961	1.147	-1.264	-1.355	0.1806	-1.636	-1.043	1.545	1.665
	0.1961	-1.765	-1.373	1.373	1.147	-1.264	-0.5213	-1.264	2.006	-1.043	-1.801	0.2249
	0.1961	-1.765	0.1961	-1.765	1.147	-1.264	1.147	-1.264	2.006	-2.095	-0.3136	0.2249
	0.1961	-1.765	-1.373	-1.765	1.147	-1.264	-2.189	-1.264	2.916	-0.5175	-0.3136	0.2249
	-1.373	-1.765	0.1961	-0.1961	-2.189	-1.264	0.3128	0.1806	0.1849	-2.095	-1.429	1.665
	-1.373	-1.765	1.765	-0.1961	-2.189	-1.264	1.981	0.1806	-0.7256	0.5339	0.4298	-2.654
	-1.373	-1.765	0.1961	1.373	-2.189	-1.264	1.147	1.625	0.1849	0.008214	-1.057	-2.654
	-1.373	-1.765	1.765	1.373	-2.189	-1.264	-0.5213	1.625	0.1849	-1.043	0.4298	-2.654
	-1.373	-1.765	-1.373	-0.1961	-2.189	-1.264	-1.355	0.1806	1.095	0.5339	0.4298	-2.654
	-1.373	-1.765	-1.373	1.373	-2.189	-1.264	-0.5213	-1.264	-2.547	0.5339	-0.6854	-1.215
	-1.373	-1.765	0.1961	-1.765	-2.189	-1.264	1.147	-1.264	-2.547	-0.5175	0.8015	-1.215
	-1.373	-1.765	-1.373	-1.765	-2.189	-1.264	-2.189	-1.264	-1.636	0.008214	-2.172	-1.215

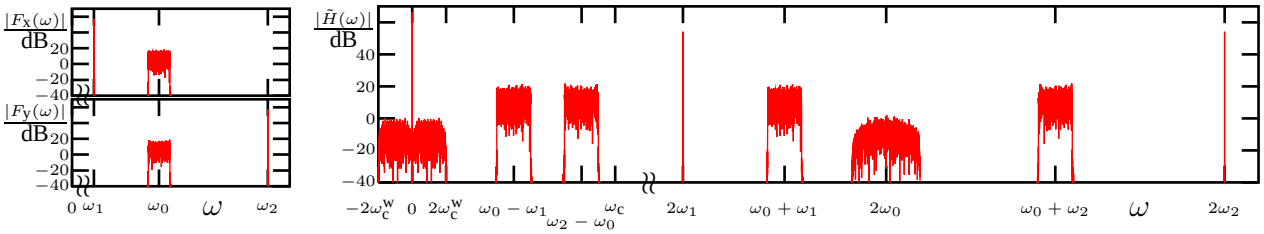

Fig. 6: Spectra $|F_x(\omega)|$ and $|F_y(\omega)|$ of $\vec{f}(t)$ and spectrum $|\tilde{H}(\omega)|$ of $R \cdot |\vec{f}(t)|^2$ for a certain bit sequence with $\omega_0 - \omega_1 = 6\omega_c^w$, $\omega_2 - \omega_0 = 10\omega_c^w$, $\omega_c = 12\omega_c^w$

independent part σ_0^2, which encloses all noise of the optical transmission line and the electrical amplification.

In Fig. 6 the Fourier spectrum $\vec{F}(\omega)$ of $\vec{f}(t)$ and the spectrum $\tilde{H}(\omega)$ of $R \cdot |\vec{f}(t)|^2$ are depicted. The two left plots represent the input spectra of the PD, the upper one is the x-polarized the lower one the y-polarized part. Obviously, the two OQAM signals are transmitted within the same frequency range around ω_0. The distances $\omega_0 - \omega_1$ and $\omega_2 - \omega_0$ are different, where ω_1 and ω_2 are the angular frequencies of the two Lasers of the heterodyne receiver. On the right hand side $|\tilde{H}(\omega)|$ is shown. In the baseband there is the spectrum of the third term in (3) plus a dc value which is a Dirac impulse at $\omega = 0$. Aside at $\omega_0 - \omega_1$ and $\omega_2 - \omega_0$ are the two QAM spectra. They are demodulated by the electrical QAM demodulator. The remaining parts above ω_c are filtered out by the PD with its cut-off frequency ω_c.

Figs. 7(a,b) show the impact of the phase noise $\varphi(t)$ in (11) on the QAM-constellation and $|\tilde{H}(\omega)|$. Ideal QAM demodulation is assumed, which means, that the carrier and clock frequencies are known. The larger Δf, the more the signal points spread out and the spectral parts of $|\tilde{H}(\omega)|$ overlap.

In Figs. 7(c,d) the impact of polarization mode dispersion (PMD) is depicted. θ is the angel between the x- and y-polarization components. For decreasing θ each signal point in Fig. 7(a) spreads out into four and thus symbol error ratio will be increased. In principle, this effect can be

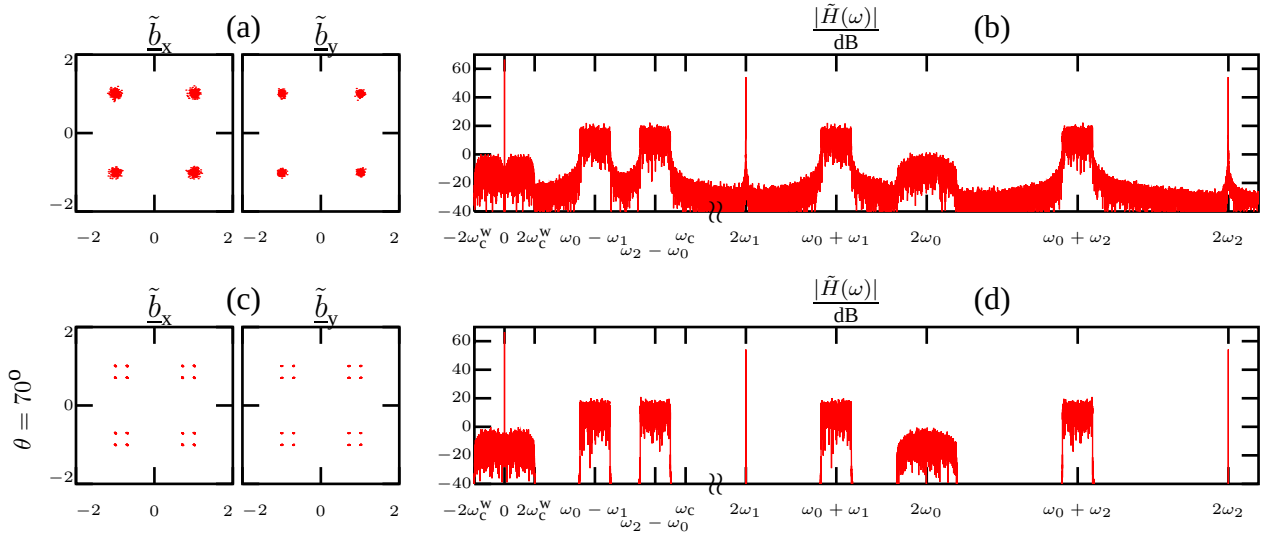

Fig. 7: (a) Constellation diagrams of $\underline{\tilde{b}}_x$ and $\underline{\tilde{b}}_y$; (b) spectrum $|\tilde{H}(\omega)|$ of $R \cdot |\vec{f}(t)|^2$ for $\Delta f = 10\,\text{MHz}$; (c) constellation diagrams of $\underline{\tilde{b}}_x$ and $\underline{\tilde{b}}_y$; (d) spectrum $|\tilde{H}(\omega)|$ of $R \cdot |\vec{f}(t)|^2$ for $\theta = 70^o$; $\omega_0 - \omega_1 = 6\omega_c^w$; $\omega_2 - \omega_0 = 10\omega_c^w$; $\omega_c = 12\omega_c^w$; bit rate $40\,\text{GHz}$

compensated partly by an equalizer. The spectrum $|\tilde{H}(\omega)|$ is nearly independent of θ, as can be seen from Fig. 7(d).

Group delay dispersion caused by β'' can be compensated at the output of the electrical QAM demodulators. The transfer function $G(\omega)$ of the squareroot raised cosine Nyquist impulse-shaping filter has to be changed to $G(\omega) \cdot \mathrm{e}^{\mathrm{j}\beta''\omega^2 z/2}$.

VI. Conclusion

We have presented a novel optical multilevel modulation scheme OQ^{2}AM which applies OQAM on two CW-Laser output signals with orthogonal polarization. One Transmitter and two receivers with heterodyne and homodyne principle are described in quite some detail. The heterodyne receiver operates with two Lasers and one PD as well as two electrically QAM demodulators. The homodyne receiver operates with four Lasers and four PD with 6 times lower cut-off frequencies. But the dynamic range of the components in the homodyne scheme is reduces by a large dc value, consequently the system performance is lowered. The additional degrees of freedom for OQ^{2}AM signal constellations compared to polarization multiplexed OQAM (PMOQAM) can be deployed to achieve a gain of about 1dB of signal to noise ratio. As an example, a 16-OQ^{2}AM is considered, yielding a spectral efficiency of $\frac{4}{(1+\beta)} \frac{\text{bit/s}}{\text{Hz}}$, where β is the roll-off factor of the Nyquist lowpass filter. The impact of phase noise of the transmit Laser is investigated, and it turns out that a full width at halve power $\Delta f = 10\,\text{MHz}$ provides a reasonable good QAM constellation diagram. It is also shown by simulation, that PMD tends to split each signal point into a group of points, thus increasing symbol error ratio.

References

[1] M. Rohde, C. Caspar, N.Heimes, M. Konitzer, E.-J. Bachus, N. Hanik, *Robustness of DPSK direcct detection transmission format in standard fibre WDM systems*, Electron. Lett. 36, pp. 1483-1484, 2000

[2] R. A. Griffin, A. C. Carter, *Optical differential quadrature phase-shift key (oDQPSK) for high capacity optical transmission*, OFC '02, WX6, Anaheim, 2002

[3] M. Ohm, J. Speidel, *Quaternary optical ASK-DPSK and receivers with direct detection*, IEEE Photonics Tech. Lett., vol.15, No.1, January 2003, pp.159-161

[4] John G. Proakis, *Digital Communications*, McGraw-Hill 4th ed. 2001

[5] Govind P. Agrawal, *Applications of Nonlinear Fiber Optics*, Academic Press 1st ed. 2001, p.139

[6] Virtual Photonics Incorporated, *Photonic Modules Reference Manual*, pp. 4-7 – 4-12 (15.11.2000).

[7] Göran Einarsson, *Principles of Lightwave Communications*, John Wiley & Sons 1st ed. 1996, p.78

[8] Gerard J. Foschini, Richard D. Gitlin and Stephen B. Weinstein *Optimization of Two-Dimensional Signal Constellations in the Presence of Gaussian Noise* IEEE Transactions on Communications, Vol. COM-22, No.1, January 1974, pp. 28-38

[9] Allen Gersho and Victor B. Lawrence *Multidimensional Signal Constellations for Voiceband Data Transmission* IEEE Journal on Selected Areas in Communications, Vol. SAC-2, No.5, September 1984, pp. 687-702

[10] Govind P. Agrawal, *Nonlinear Fiber Optics*, Academic Press 3th ed. 2001, p.9

[11] E. Voges and K. Petermann (Hrsg.), *Optische Kommunikationstechnik*, Springer-Verlag 1th ed. 2002, p.26